Xu-Jie Lu, Xue-Fei Zhou, Zheng-Liang Zhu, Yali Sun, Kai Tang, Fu-Hou Lei, Zu-Guang Liu, Ting Wang

CATALYTIC OXIDATION OF LIGNIN TO AROMATICS OVER SALEN-PORPHYRIN COMPLEX AS A BIOMIMETIC CATALYST

The aim of this work is to enable increased production of aromatics by the use of salen-porphyrin complex (ZnPSC$_6$) as a binuclear catalyst for the catalytic oxidation of Indulin AT lignin. Catalytic activity was enhanced by the increase in active sites, as confirmed by the results observed in the conversion of lignin model compounds and Indulin AT lignin compared with processes using the mononuclear complexes Zn(salen) and Zn(Phe-TPP). The yields of long and convoluted aromatics from the catalytic oxidation of Indulin AT lignin with ZnPSC$_6$ reached high values after reaction at 80°C for 24 h. Notably, the formation of vanillin was promoted by the increase in active sites over ZnPSC$_6$. This was followed by a significant decrease of β-O-4 linkages and refractory condensed substructures in the lignin, induced by ZnPSC$_6$. This may be expected to be an important area for further study.

Keywords: lignin, biomimetic catalysis, mononuclear complex, binuclear complex, lignin structure

Introduction

In recent years, the efficient conversion of lignin has attracted increasing attention due to the shortage of resources. The key focus is on finding highly active catalysts to transform lignin, where lignin can be degraded efficiently and selectively to obtain high yields of the degradation products [Teguia et al. 2017].

Xu-Jie Lu (*xujie_lu@163.com*), Hainan Tropical Ocean University, Sanya, China; Xue-Fei Zhou (*lgdx602@sina.com*), Fuzhou University，Fuzhou, China; Nankai University, Tianjin, China; Wuyi University, Wuyishan, China; Kunming University of Science and Technology, Kunming, China; Tsinghua University, Beijing, China; Qilu University of Technology, Jinan, China; Zheng-Liang Zhu (*zhlzhu@163.com*), Kunming University of Science and Technology, Kunming, China; Yali Sun✉ (*sonaly@126.com*), Hainan Tropical Ocean University, Sanya, China; Chongqing University Chongqing, China; Sichuan University of Science and Engineering, Zigong, China; Kai Tang (*13795585046@163.com*) Sichuan University of Science and Engineering, Zigong, China; Fu-Hou Lei (*leifuhou@163.com*), Zu-Guang Liu (*674841591@qq.com*), Ting Wang (*ting071116@qq.com*), Guangxi University For Nationalities, Nanning, China

Salen complexes have been widely used as catalysts in the oxidation of lignin and lignin model compounds [Diaz-Urrutia et al. 2016; Ma et al. 2017]. In the oxidation reactions, phenoxy radical complexes are formed and then react with lignin to form phenoxy radicals, in which free radical coupling occurs to give various compounds such as alkyl phenyl ketones, benzoic acids, cinnamic aldehydes, benzofurans and other compounds [Badamali et al. 2011; Zhou, 2015]. Metalloporphyrins have active centers similar to those of lignin peroxidase (LiP) and manganese peroxidase (MnP) which catalyze the oxidation of C–C, C–O and 5–5' bonds in the lignin structure [Zhu et al. 2015]. Maruyama et al. [1990] used salen-porphyrin binuclear complexes as active site models of metalloenzymes, and found that they had an advantage over salen or porphyrin complexes in catalytic performance. In fact, it was observed by Su et al. [2007] that the increase in the active sites in the binuclear complex resulted in a proportional increase in cyclohexane conversion (12.45%) compared with salen (4.07%) or porphyrin complex (5.05%). Wezenberg et al. [2009] prepared supramolecular hybrid assemblies between metallosalen and metalloporphyrin components via Zn-Npyr coordination using a one-pot procedure, and demonstrated by NMR spectroscopy and MALDI-TOF mass spectrometry that there were two active sites in the supramolecular complex. Xia et al. [2015] indicated that the binuclear complexes exhibited better catalytic performance than cobalt(III)-based porphyrin and salen catalysts in epoxidation.

Salen-porphyrin binuclear complexes have drawn great attention due to their readily modifiable nature and promising catalytic behavior, such as high selectivity and good efficiency for catalysis with respect to the transformation of organic compounds. It was hence expected that the optimal combination of salen and porphyrin complex used for the enhancement of the catalytic reaction might lead to maximum lignin degradation and high selectivity. To the authors' best knowledge, there are no similar studies described in the literature. The objective of this work was to study the increase in aromatics production in lignin conversion catalyzed by the salen-porphyrin binuclear complex.

Materials and methods

Materials

Guaiacylglycerol-β-guaiacyl ether, a β-O-4 lignin dimer, was synthesized following the procedure previously reported [Song et al. 2012]. ^{1}H-NMR (500 MHz, DMSO-d_6): δ 7.63 (dd, 1H, J_1 = 8.38 Hz, J_2 = 2.11 Hz, Ar-H), 7.52 (d, 1H, J = 2.13 Hz, Ar-H), 6.94 (d, 1H, J = 8.42 Hz, Ar-H), 4.38 (s, 2H, CH_2), 3.95 (s, 3H, CH_3O), 3.93 (s, 3H, CH_3O).

Indulin AT lignin, a kraft lignin, was obtained from Sigma Aldrich.

Chloroform (Sinopharm Chemical Reagent Co., Ltd) was dried with $NaHCO_3$ and $CaCl_2$ and distilled prior to use. Other chemicals used (Sinopharm

Chemical Reagent Co., Ltd) were analytical grade chemicals. Milli-Q ultra-pure water was used in all experiments.

Synthesis of salen-porphyrin complex

The salen-porphyrin complexes were synthesized following the protocol previously described [Zhao et al. 2006].

HPTPP (5,10,15-triphenyl-20-p-hydroxyl phenyl porphyrin): *p*-Hydroxyl benzaldehyde (23 g) and benzaldehyde (57 ml) were dissolved in propionic acid (2000 ml), and stirred in a three-neck flask at 140°C for 20 min. Pyrrole (52 ml) was then slowly added, and the reaction continued at 130°C for 30 min. Afterwards the mixture was left for 12 h at room temperature without agitation, half of the propionic acid was removed in vacuum by a rotary evaporator, and then the same amount of ethanol was added. After 24 h, the mixture was filtered to obtain a precipitate. The precipitate was washed with ethanol, dried under vacuum and purified with chloroform in a neutral alumina column. The second band was then taken to obtain the HPTPP. The HPTPP was concentrated in vacuum and purified with a mixture of chloroform and ligarine (1:1) in a neutral alumina column.

Salen-OH: Salicylaldehyde (630 mg), o-phenylenediamine (560 mg) and 2,5-dihydroxybenzaldehyde (700 mg) were dissolved in chloroform (60 ml) and stirred at room temperature for 20 h. After that, a yellow precipitate was formed, and the solution was orange red. After the precipitate was filtered, the solution was concentrated in vacuum and purified by column chromatography, and the second band was taken to obtain salen-OH. The salen-OH was concentrated and purified with a silica gel column.

Salen$(CH_2)_6$Br: The salen-OH ligand (0.25 mmol) and Br$(CH_2)_6$Br (2.5 mmol) were dissolved in acetone (20 mL), and anhydrous potassium carbonate (3.75 mmol) was added. The mixture was refluxed in darkness for 5 h, concentrated in vacuum, and then extracted with chloroform. The organic layers containing salen$(CH_2)_6$Br were collected, dried with anhydrous sodium carbonate and purified with chloroform by column chromatography.

HPTPP-$(CH_2)_6$-salen (HPSC$_6$): Anhydrous potassium carbonate was added to acetone, followed by the addition of HPTPP and salen$(CH_2)_6$Br. The reaction was carried out at room temperature for 17 h while avoiding exposure to sunlight. After that, the mixture was concentrated in vacuum, extracted with chloroform and washed with ultrapure water to remove inorganic matter. The organic phases were collected and dried with anhydrous sodium sulphate. The crude HPSC$_6$ was purified with a silica gel column using chloroform as eluent.

ZnPTPP-$(CH_2)_6$-salenZn (ZnPSC$_6$): HPSC$_6$ was refluxed in chloroform for 10 min, zinc acetate was added, and the mixture was refluxed for 5 h. It was then dried with anhydrous sodium sulphate and purified by chloroform in a silica gel column to obtain ZnPSC$_6$.

The whole process was carried out in a nitrogen atmosphere.

ZnPSC$_6$ (fig. 1): Zn$_2$C$_{70}$H$_{52}$N$_6$O$_4$, 66.28% C (66.07%), 4.21% H (4.11%), 6.73% N (6.51%). ^{1}H-NMR (CDCl$_3$): (CH$_2$)$_n$, 1.242-1.653; -O-CH$_2$, 3.413; P-O-CH$_2$, 4.196; -phenyl, 7.263-7.295; -phenyl 3, 5/-phenyl 3', 5', 7.772-7.875; -phenyl 2, 6/-phenyl 2', 6', 8.113-8.206; -C=N, 8.598/8.60l; -Pyrrole-H, 8.87-8.94.
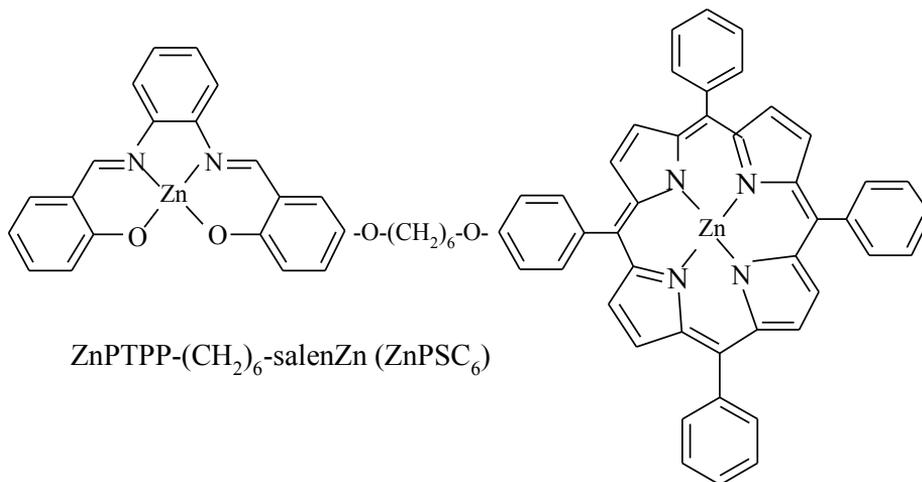

ZnPTPP-(CH$_2$)$_6$-salenZn (ZnPSC$_6$)

Fig. 1. ZnPSC$_6$

Synthesis of Zn(salen) complex

The salen was prepared by condensation reactions of ethylenediamine with salicylaldehyde in methanol. The metal complex was synthesized from the salen and a slight excess of zinc acetate by refluxing.

Synthesis of zinc porphyrin (Zn(Phe-TPP))

N-chloroacetyl phenylalanine and 5-(p-hydroxylphenyl)-10,15,20-tris(p--chlorophenyl) porphyrin were synthesized according to the procedures previously described [Huang et al. 1983]. They were then subjected to an equimolar reaction in DMF in the presence of pyridine and potassium carbonate to obtain 5-p-(N-phenylalanine formyl methoxyl) phenyl-10,15,20-tris(p--chlorophenyl) porphyrin (Zn(Phe-TPP)), and purified using neutral alumina column chromatography, followed by refluxing for 30 min in the presence of zinc acetate in DMF. After cooling to room temperature, the precipitate was filtered, dried, purified by alumina column chromatography, and finally recrystallized in chloroform-ethanol to obtain Zn(Phe-TPP). Zn(Phe-TPP) (fig. 2), ZnC$_{55}$H$_{36}$O$_4$N$_5$Cl$_3$, 65.37% C (65.88%), 3.46% H (3.62%), 6.35% N (6.98%). FTIR: -COOH, 1724 cm^{-1}; porphyrin ring, 1005 cm^{-1}; C-N, 1485 cm^{-1};

benzene ring in tetraphenyl porphyrin, 1593/1021/1002/880 cm^{-1}; porphyrin skeleton, 1546/1476/1242/1056 cm^{-1}; zinc porphyrin, 1365 cm^{-1}. ^{1}H-NMR (CDCl$_3$): 8H/Ph-NH$_2$, 5.61; 8H/m-ArH, 6.73-7.47; 8H/O-ArH, 7.62–8.42; 8H/β--pyrrole, 8.93.
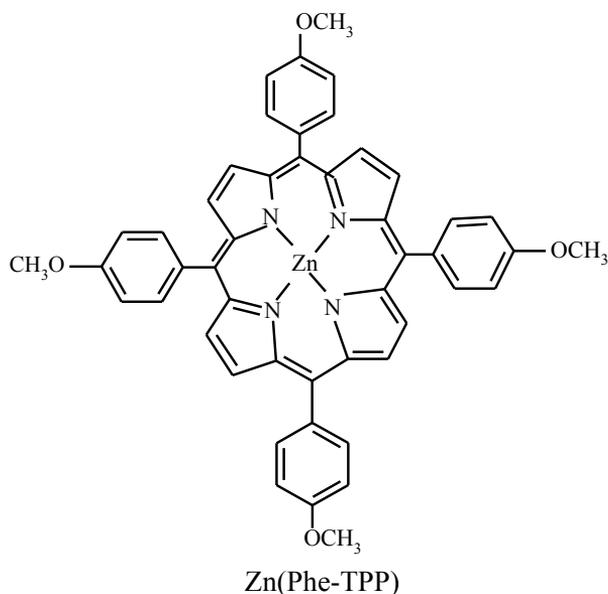

Zn(Phe-TPP)

Fig. 2. Zn(Phe-TPP)

Catalytic reactions

Indulin AT lignin (36 mg) or lignin model compound (1.0 mM) was used as the substrate, which was fully dissolved in sodium hydroxide aqueous solution (60 mL, pH 9.0), and ZnPSC$_6$, Zn(salen) or Zn(Phe-TPP) (3 mg) was employed as the catalyst in the reaction. The reaction was performed under stirring in sealed vials at 80°C for Indulin AT lignin or 25°C for lignin model compound, using air as oxidant, by bubbling from the headspace. The control trial was conducted under the same conditions without the addition of catalyst.

After the reaction, the catalyst was recovered by centrifugation and washed with ultrapure water, followed by drying under reduced pressure. The aqueous solution was adjusted to pH 2.0 with hydrochloric acid (0.2 M), and the residual lignin obtained was dried at 50°C in vacuum for GPC and ^{31}P-NMR analysis. Next the aqueous solution was extracted with ether (3 × 10 mL), and the ether phase was concentrated to 5 mL at 30°C in vacuum for GC/MS analysis.

GC-MS

The ether phase containing the degradation products from Indulin AT lignin or lignin model compound was characterized using an Agilent HP6890-5973 GC-

-MS instrument, equipped with a mass selective detector and a capillary column (30 m × 0.25 mm × 0.25 μm). Helium was used as the carrier gas. The temperature was ramped from 40°C to 280°C at 10°C/min (held for 5 min). Compounds were quantitatively identified using benzaldehyde as the internal standard, based on the NIST 2005 MS library. Replicates were performed and better reproducibility was obtained, with a coefficient of variation less than 3%.

FTIR

FTIR spectra of lignin samples were obtained using a Bruker Equinox 55 FTIR spectrometer.

Quantitative ^{31}P-NMR

Quantitative ^{31}P-NMR spectra were obtained on a Bruker DRX500 MHz spectrometer for lignin samples derivatized with 2-chloro-4,4,5,5-tetramethyl--1,3,2-dioxaphospholane (TMDP). The functional groups in the 31P-NMR spectra were quantified based on the internal standard (cyclohexanol) [Michael and Arthur 2001; Pu et al. 2011].

Molecular weight analysis

The molecular weight of the acetylated lignin was measured in tetrahydrofuran using Agilent 1100 GPC. Acetylation of the lignin samples was performed with acetic anhydride and pyridine [Thring et al. 2002].

Results and discussion

Catalytic degradation of lignin model compound

The catalytic oxidation of β-O-4 model compound was performed using the previously described catalysts. The degradation products obtained are shown in Scheme 1. It was observed that ZnPSC$_6$ was the most active catalyst, followed by Zn(Phe-TPP) and Zn(salen), with degradation rates of 43%, 37% and 34% respectively, in the degradation of the dimer at 25°C (fig. 3). In addition, it can be concluded that the dimer was degraded by β-O-4 cleavage and benzylic oxidation, as confirmed respectively by product 1 and by products 2 and 3. Similar results were reported previously by Dawange et al. [2015].
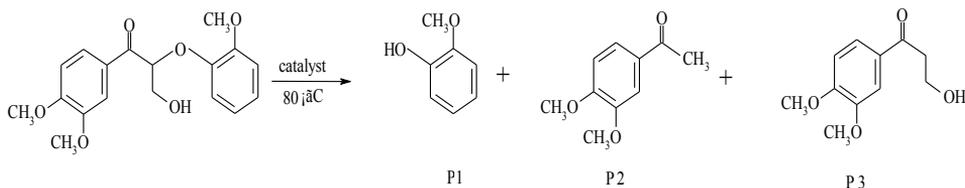
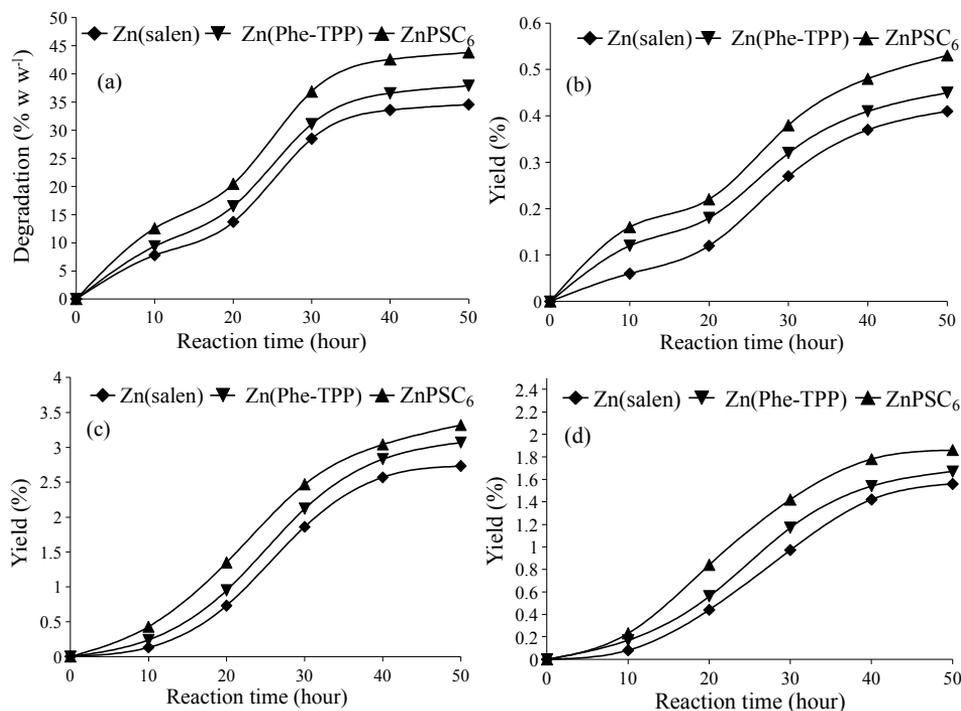**Scheme 1. Catalytic degradation of β-O-4 lignin model compound**

Fig. 3. Degradation of β-O-4 lignin dimer. (a) Degradation rate of lignin dimer, (b) yield of product 1, (c) yield of product 2, (d) yield of product 3

Catalytic degradation of Indulin AT lignin

The catalytic oxidation of Indulin AT lignin mainly yielded five aromatic compounds: vanillin (product 1), 2-methoxy phenol (product 2), 4-hydroxy-3--methoxyacetophenone (product 3), phenol (product 4) and 4-hydroxy-3--methoxy benzoic acid (product 5). Vanillin was the main compound among the degradation products, as shown by their respective yields in figure 4. The control test showed negligible oxidation of the Indulin AT lignin, whereas $ZnPSC_6$ demonstrated a significant promotional effect on lignin degradation at room temperature when compared with the other two catalysts (fig. 4). For example, $ZnPSC_6$ produced a vanillin yield of 8.80% by weight with respect to lignin, compared with 3.43% for Zn(Phe-TPP) and 2.54% for Zn(salen), since the structure of ZnPSC6 provided more active sites for regulating the catalytic reaction by abstracting phenolic hydrogen atoms to produce phenoxy radicals by oxo-complex [Maruyama et al. 1991; Fujii et al. 2003]. Another explanation is that it achieves high catalytic selectivity by mimicking an enzyme [Höcker et al. 2004; Martin and Teixeira 2013]. Thus, $ZnPSC_6$ is of interest, as a high yield of vanillin was obtained in lignin conversion compared with the results for

biological enzymes and chemical catalysts [Strassberger et al. 2011; Li et al. 2015; Zhou and Tang 2016; Mishra et al. 2017].
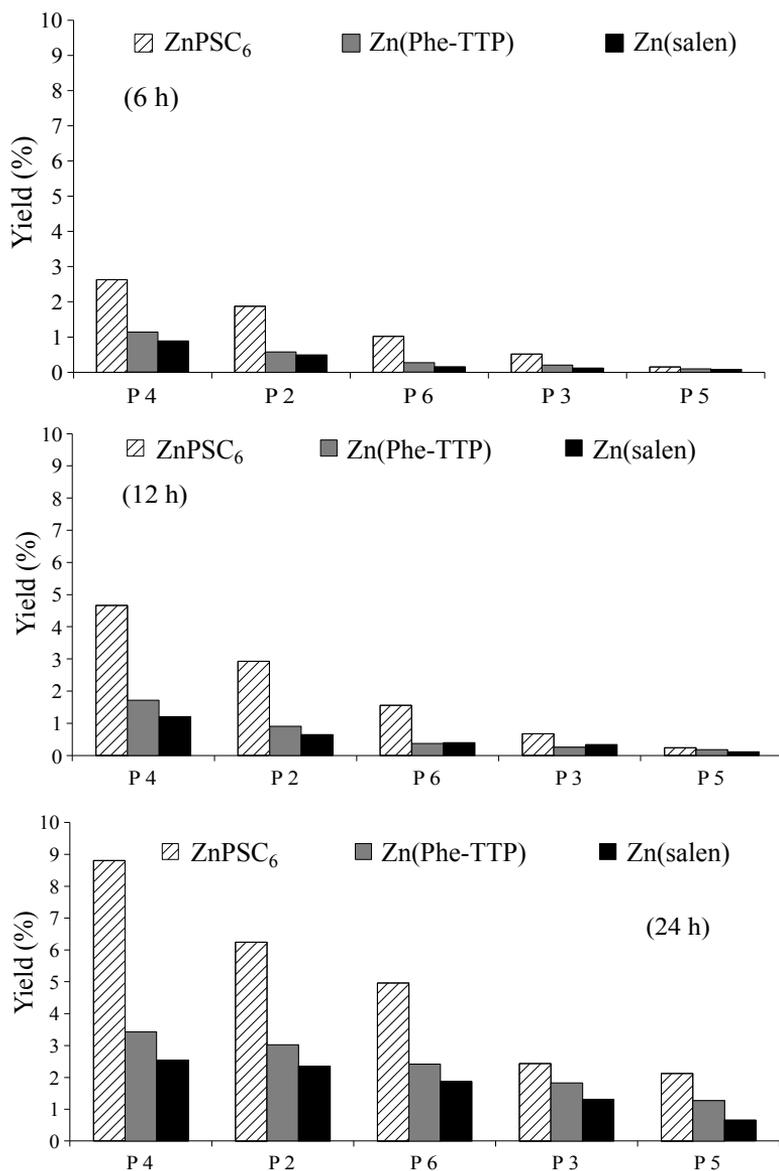

Fig. 4. Yield of aromatic compound

In addition, recycling tests were carried out for the catalysts to assess their stability on reuse. The results are shown in figure 5. It was found that the activity of $ZnPSC_6$ decreased after 10 recycling times, while that of Zn(salen) and Zn(Phe-TPP) fell after 6 recycling times (according to the evolution of vanillin),

indicating that the binuclear complex was more stable than the mononuclear complex.
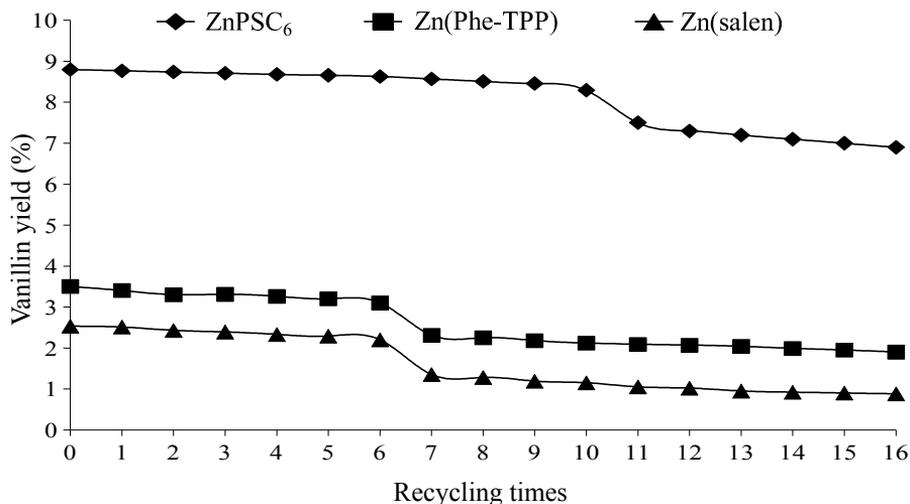
Fig. 5. Vanillin yield vs. recycling times in oxidation of lignin for 24 h

Structural characterization of lignin

The structure of the lignin samples was determined to map the progress of the catalytic reaction with GPC, FTIR and 31P-NMR. The molecular weights (table 1) showed that catalysis led to the decomposition of lignin, which may be explained by the cleavage of some of the linkages in lignin, such as β-O-4 [Neumann et al. 2014]. Simultaneously, according to the molecular weight data, $ZnPSC_6$ exhibited superiority in lignin degradation over Zn(salen) and Zn(Phe--TPP). This is due to its binuclear features, which combine the advantages of Zn(salen) and Zn(Phe-TPP).

Table 1. Molecular weight of lignin samples by GPC analysis

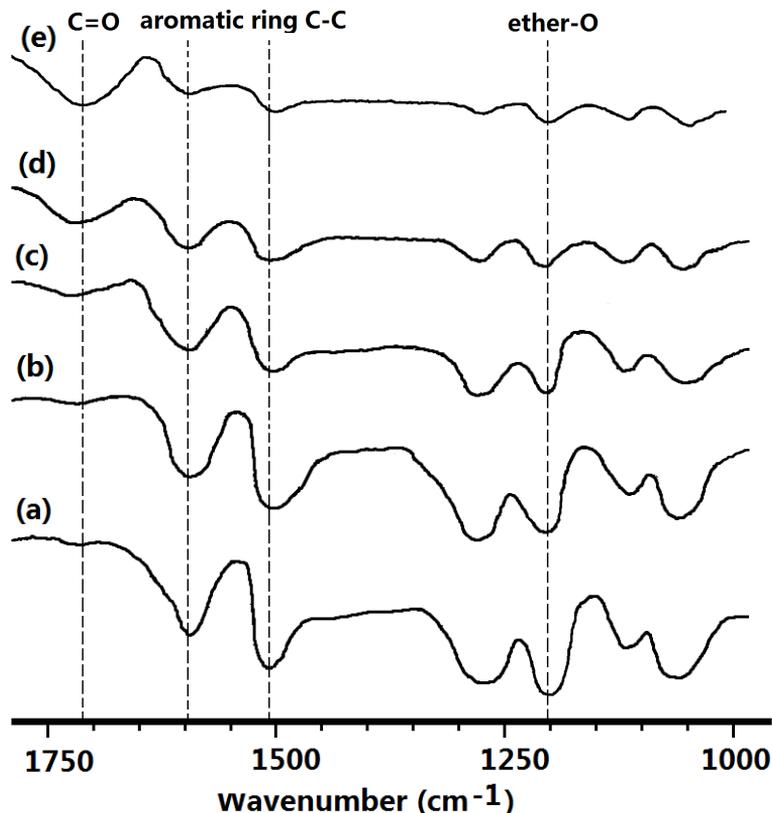| Reaction time [h]	Mw [g·mol⁻¹]			
	Control	Zn(salen)	Zn(Phe-TPP)	$ZnPSC_6$
6	3103	2977	2774	2196
12	2876	2674	2238	1764
24	2354	2086	1765	1262

Mw of Indulin AT lignin: 3127.

Fig. 6. FTIR spectra of lignin samples. (a) Indulin AT lignin; (b) residual lignin from the control; (c) residual lignin from catalysis by ZN(salen); (d) residual lignin from catalysis by Zn(Phe-TPP); (e) residual lignin from catalysis by ZnPSC$_6$

The lignin samples obtained from the catalytic reaction were also analyzed by FTIR (fig. 6). Interestingly, the oxidation of the side chain in lignin was confirmed by the increasing intensity of carbonyl (1720 cm^{-1}) with catalysis, which was accompanied by a decrease in the aliphatic OH content (table 2) as determined by ^{31}P-NMR [Crestini et al. 1999]. This is consistent with the biodegradation of lignin [Fackler et al. 2006; Nousiainen et al. 2014; de Gonzalo et al. 2016]. The formation of 1,2-butanediol found in the catalytic oxidation of lignin was also supported by the decrease in the aromatic ring vibration bands at 1506 cm^{-1} and 1558 cm^{-1} with the progression of Zn(salen), Zn(Phe-TPP) and ZnPSC$_6$ treatment, versus the control. Meanwhile, FTIR analyses further confirmed the change of β-O-4 in the lignin. According to the FTIR spectra shown in figure 6, catalysis weakened the ether-O linkage, which was crucial for lignin fragmentation, resulting in an increase in the content of phenolic OH [Kim et al. 2016], especially for ZnPSC$_6$ as compared with the mononuclear complexes (table 2).

Table 2. Content of functional groups by ^{31}P-NMR analysis

Chemical shift (ppm)	Functional group	Content [mmol·g^{-1}]				
		Indulin AT lignin	Control	Catalysis		
				Zn(salen)	Zn(Phe-TPP)	ZnPSC$_6$
154.2–153.4	Internal standard	–	–	–	–	–
149.6–145.7	Aliphatic hydroxyl group	1.63	1.47	1.14	1.02	0.66
144.3–140.5	Condensed phenolic hydroxyl group	0.71	0.56	0.33	0.21	0.08
143.2–142.4	Phenolic hydroxyl group in syringyl structure	0.22	0.37	0.66	0.84	1.27
140.3–138.5	Phenolic hydroxyl group in guaiacyl structure	0.18	0.27	0.47	0.63	0.97
138.7–137.3	*p*-Phenolic hydroxyl group	0.14	0.26	0.52	0.68	1.07
136.3–133.5	Hydroxyl group in carboxyl group	0.13	0.38	0.63	0.73	1.12

Notably, the lignin degradation induced by ZnPSC$_6$ resulted in a significant decrease in the content of refractory condensed phenolics, compared with degradation by Zn(salen) and Zn(Phe-TPP) (table 2). This was an important factor enhancing lignin decomposition by the binuclear complex.

Conclusions

Salen-porphyrin complex (ZnPSC$_6$) was successfully used as a biomimetic catalyst in the conversion of lignin to aromatics. ZnPSC$_6$ displayed outstanding performance in the catalytic oxidation of lignin model compounds and Indulin AT lignin compared with the mononuclear complexes Zn(salen) and Zn(Phe--TPP). The degradation products were tracked using GC-MS, and the structural changes in the degradation of lignin were characterized by GPC, FTIR and ^{31}P-NMR, to examine the catalytic effect of the binuclear complex. Consideration should hence be given to further research concerning the catalytic mechanism in lignin conversion using salen-porphyrin complex as catalyst.

References

Badamali S.K., Luque R., Clark J.H., Breeden S.W. [2011]: Co(salen)/SBA-15 catalysed oxidation of a β-O-4 phenolic dimer under microwave irradiation. Catalysis Communications 12 [11]: 993-995

Crestini C., Saladino R., Tagliatesta P., Boschi T. [1999]: Biomimetic degradation of lignin and lignin model compounds by synthetic anionic and cationic water soluble manganese and iron porphyrins. Bioorganic & Medicinal Chemistry 7 [9]: 1897-1905

Dawange M., Galkin M.V., Samec J.S.M. [2015]: Selective aerobic benzylic alcohol oxidation of lignin model compounds: route to aryl ketones. ChemCatChem 7 [3]: 401--404

de Gonzalo G., Colpa D.I., Habibm M.H.M., Fraaije M.W. [2016]: Bacterial enzymes involved in lignin degradation. Journal of Biotechnology 236: 110-119

Diaz-Urrutia C., Hurisso B.B., Gauthier P.M.P., Sedai B., Singer R.D., Baker R.T. [2016]: Catalytic aerobic oxidation of lignin-derived bio-oils using oxovanadium and copper complex catalysts and ionic liquids. Journal of Molecular Catalysis A: Chemical 423: 414-422

Fackler K., Gradinger C., Hinterstoisser B., Messner K., Schwanninger M. [2006]: Lignin degradation by white rot fungi on spruce wood shavings during short-time solid--state fermentations monitored by near infrared spectroscopy. Enzyme and Microbial Technology 39 [7]: 1476-1483

Fujii H., Kurahashi T., Ogura T. [2003]: A sterically hindered salen iron complex as a model for active sites of mononuclear non-heme iron enzymes. Journal of Inorganic Biochemistry 96 [1]: 133-133

Höcker B., Claren J., Sterner R., Petsko G.A. [2004]: Mimicking enzyme evolution by generating new (β α)8-barrels from (β α)4-half-barrels. Proceedings of the National Academy of Sciences of the United States of America 101 [47]: 16448-16453

Huang S., Sun L., Ye C. [1983]: Studies on the porphyrin compounds. Journal of the Chinese Chemical Society (Chinese Edition) 4 [l]: 381-384

Kim H.-Y., Jang S.-K., Hong C.-Y., Choi J.W., Choi I.-G. [2016]: Relationship between characteristics of ethanol organosolv lignin and the productivity of phenolic monomers by solvolysis. Fuel 186: 770-778

Li W., Zhang M., Du Z., Ma Q., Jameel H., Chang H.-M. [2015]: Photocatalytic degradation of lignin model compounds and kraft pine lignin by CdS/TiO$_2$ under visible light irradiation. Bioresources 10 [1]: 1245-1259

Ma Q.Y., Liu K.J., Mao J.Y., Chen K.X., Liang C., Yao J., Chen Z.R., Li H.R. [2017]: Kinetic studies on the liquid-phase catalytic oxidation of 4-methyl guaiacol to vanillin. The Canadian Journal of Chemical Engineering 95 [8]: 1544-1553

Maruyaama K., Kobayashi F., Osuka A. [1990]: Salen-capped porphyrins as an active site model of metalloenzymes: Synthesis and their intramolecular interactions between the metal complexes. Bulletin of the Chemical Society of Japan 63 [9]: 2672-2681

Maruyama K., Kobayashi F., Osuka A. [1991]: Synthesis and characterization of directly linked salen–porphyrin system with constrained geometries. Bulletin of the Chemical Society of Japan 64 [1]: 29-34

Michael Z., Arthur R. [2001]: N-hydroxy compounds as new internal standards for the ^{31}P-NMR determination of lignin hydroxyl functional groups. Holzforschung 55 [3]: 283-285

Mishra V., Jana A.K., Jana M.M., Gupta A. [2017]: Enhancement in multiple lignolytic enzymes production for optimized lignin degradation and selectivity in fungal pretreatment of sweet sorghum bagasse. Bioresource Technology 236: 49-59

Martin C.S.M., Teixeira F.S. [2013]: Electrochemical properties of oxo–manganese complex biomimicking enzyme active sites and its electrocatalytic application for dopamine determination. Electrocatalysis 4 [2]: 92-100

Neumann G.T., Pimentel B.R., Rensel D.J., Hicks J.C. [2014]: Correlating lignin structure to aromatic products in the catalytic fast pyrolysis of lignin model compounds containing β-O-4 linkages. Catalysis Science & Technology 4 [11]: 3953-3963

Nousiainen P., Kontro J., Manner H., Hatakka A., Sipilä J. [2014]: Phenolic mediators enhance the manganese peroxidase catalyzed oxidation of recalcitrant lignin model compounds and synthetic lignin. Fungal Genetics and Biology 72: 137-149

Pu Y., Cao S., Ragauskas A.J. [2011]: Application of quantitative 31P NMR in biomass lignin and biofuel precursors characterization. Energy & Environmental Science 4 [9]: 3154-3166

Song Q., Wang F., Xu J. [2012]: Hydrogenolysis of lignosulfonate into phenols over heterogeneous nickel catalysts. Chemical Communications 48 [56]: 7019-7021

Strassberger Z., Tanase S., Rothenberg G. [2011]: Reductive dealkylation of anisole and phenetole: towards practical lignin conversion. European Journal of Inorganic Chemistry 2011 [27]: 5246-5249

Su J.-L., Zhao W.-J., Zhang F.-C., Gao L.-Z., Gao L. [2007]: Study of complexes of salen--porphyrin. Applied Chemical Industry 36 [4]: 390-393

Teguia C.D., D'Amours S., Albers R., Stuart P. [2017]: Decision-making process for the identification of preferred lignin-based biorefinery strategies. TAPPI Journal 16 [4]: 229--240

Thring R.W., Chornet S., Bouchard J., Vidal P.F., Overend R.P. [2002]: Characterization of lignin residues derived from the alkaline hydrolysis of glycol lignin. Canadian Journal of Chemistry 68 [1]: 82-89

Wezenberg S.J., Metselaar G.A., Escudero-Adán E.C., Benet-Buchholz J., Kleij A.W. [2009]: Access to hybrid supramolecular salen-porphyrin assemblies via a selective in situ transmetalation-metalation self-assembly sequence. Inorganica Chimica Acta 362 [4]: 1053-1057

Xia W., Salmeia K.A., Vagin S.I., Rieger B. [2015]: Concerning the deactivation of cobalt(III)-based porphyrin and salen catalysts in epoxide/CO_2 copolymerization. Chemistry: A European Journal 21 [11]: 4384-4390

Zhao X.-J., Ruan W.-J., Zhu Z.-A. [2006]: Study on synthesis and spectral properties of porphyrin-salen compounds. Chinese Journal of Organic Chemistry 26 [8]: 1087-1092

Zhou X.-F. [2015]: Catalytic oxidation and conversion of kraft lignin into phenolic products using zeolite-encapsulated Cu(II) [H_4]salen and [H_2]salen complexes. Environmental Progress & Sustainable Energy 34 [4]: 1120-1128

Zhou X.-F., Tang K. [2016]: Combining laccase with Cu(salen) catalysts for oxidation of kraft lignin. Drewno 59 [198]: 35-47

Zhu C., Ding W., Shen T., Tang C., Sun C., Xu S., Chen Y., Wu J., Ying H. [2015]: Metallo-deuteroporphyrin as a biomimetic catalyst for the catalytic oxidation of lignin to aromatics. ChemSusChem 8 [10]: 1768-1778